CFD Letters

CFD Simulation Model for Optimum Design of B-Series Propeller using Multiple Reference Frame (MRF)

Niki Veranda Agil Permadi[1,*], Erik Sugianto[2]

[1]   Department of Systems & Naval Mechatronic Engineering, National Cheng Kung University, Taiwan
[2]   Department of Marine Engineering, Hang Tuah University, Indonesia

ARTICLE INFO	ABSTRACT
              	Propulsion system is one of ship systems which require more attention, especially on propeller design. The propeller design greatly affects the ship speed. It is expected to be able to have maximum value of thrust coefficient and efficiency. Hence, the optimum design of propeller can be obtained by multi objective optimization process. In this study, a preliminary optimization is applied to B-series propeller with the Non-dominated Sort Genetic Algorithm-II (NSGA-II). The purpose of this study is to find out the optimum performance of B-series propeller. The thrust coefficient and open water efficiency are maximized in the optimization process which are then subjected to constraint function imposed by required thrust. The optimization is carried out to blade number Z=3 and Z=5. The population of design space is obtained after running the optimization program. The final optimum design parameter is considered using crowding distance value in the population. The result obtained by NSGA-II showed that the optimum design for Z=3 are B3-787, B3-314, B3-560, and Z=5 are B5-416, B5-501, B5-476 respectively. In addition, the Computational Fluid Dynamics analysis (CFD) is employed to investigate the characteristic of each propeller model by using Multi Reference Frame (MRF) approach. The CFD results showed that the highest thrust value of the Z=3 is 172.38 kN generated by the B3-787 whereas the highest thrust value of Z=5 is 168.80 kN generated by the B5-501 model.

1. Introduction

One of particular concern of ship propulsion system is the propeller. There are various parameters which affect the propeller performance, such as propeller blade number (Z), propeller diameter (D), blade area ratio (A_E/A_O), pitch ratio (P/D), and propeller rotation (N). Those parameters affect the value of the thrust coefficient (K_T), torque coefficient (K_Q), and propeller efficiency (η) greatly. As a result, these values will influence the propeller performance in converting the main engine power into thrust to move the ship at a certain speed. The problem which is often encountered by propeller designer is determining the appropriate propeller configuration for the ship's requirement. The propeller must be able to have maximum value of thrust coefficient and

---

efficiency simultaneously. Thus, the optimum design of propeller can be obtained by multi objective optimization process. The multi objective optimization method is able to provide several alternative solutions to a problem with more than one objective function. Such as propeller design problems where the propeller must be able to provide the best performance. Propeller characteristics are expressed in terms of thrust coefficient (K_T) and open water efficiency (η_O). These values are considered as objective functions in the propeller design optimization. By formulating the constraint function, the optimal parameters of the propeller geometry will be obtained. As a result, the propeller will be able to provide optimal thrust coefficient (K_T) and open water efficiency (η_O) values simultaneously.

Various study had been carried out to deal with the multi objective optimization problem. Ehsan *et al.* [1] discussed a design methodology to optimize the relationship between the hull and propeller simultaneously using the evolutionary algorithm method. In this study, the Life Time Consumption (LFC) function and the cost function including thrust, torque, and propeller efficiency were determined as the objective functions. The results showed that the method used was appropriate and effective for the optimization of propeller design. Then, ship hull–propeller system optimization based on the multi-objective evolutionary algorithm using NSGA-II revealed that the proposed method is an appropriate and effective approach for finding Pareto optimal solutions distributed uniformly and is able to improve both of the objective functions significantly, lifetime fuel consumption (LFC) and lifetime cost function (Cost) [2]. Similar to the research, Jiang *et al.*, [3] introduced a new approach to optimize the propeller design by considering fluid-structure interaction. The proposed method was effective for optimizing propeller design and was able to minimize unsteady force of propeller. Benini Ernesto [4] developed a multi objective optimization for B-screw series propellers with the objective of optimizing the thrust coefficient (K$_T$) and propeller efficiency (η) using an evolutionary algorithm method. The results showed that the evolutionary algorithm was quite robust to generate optimum design. Xie [5] also developed an initial optimization method in propeller design with a multi objective optimization approach in the form NSGA-II with the aim of optimizing the value of the thrust coefficient (K_T) and propeller efficiency (η). The results of his research were one set of Pareto solution which stated the optimal solution population which can be used as a propeller design parameter. However, the study was not proposed to optimize the propeller for each blade number. Gaafary *et al.*, [6] developed a program to optimize the B-series propeller type design. This research was performed with only one objective function and the other objectives were formulated as constraint. The program was able to generate optimum design of propeller and the results were quite close to those generated by commercial optimization software. Takekoshi *et al.*, [7] proposed the optimization program for the design of the propeller blade section. By this method, the propeller efficiency was improved by 1.2% under the constrains of constant thrust and a prescribed margin for face cavitation. A matching optimization method of ship engine and propeller based on hybrid program combined from particle swarm optimization (PSO) and genetic algorithms (GA) is developed by Ren and Zhang [8]. The study showed that the hybrid approach was able to increases the diversity of particles and was significantly efficient.

The computational fluid dynamics (CFD) is commonly used to investigate the performance of a propeller. Some CFD approaches for rotating body such as water turbine has been widely developed [9]. The Arifin *et al.* [10] proposed tubercle propeller analyzed by CFD, the results shows the tubercle shape reduces the total pressure at the propeller blade, especially at the edges. Prakoso *et al.*, [11] compared the moving mesh method with the six degrees freedom (6-DOF) UDF method for simulation of cross-flow turbines at the pico scale in 2D domain. The results showed that 6-DOF method was more accurate than the moving mesh method for predicting the performance of cross-flow turbines at the pico scale. However, the moving mesh method was superior in term of

convergence rate. Next, the assessment of turbulence modelling for numerical simulations into pico hydro turbine was conducted by Adanta *et al*., [12]

Regarding the convergence and grid independence, the application of the Grid Convergency Index (GCI) method and courant number analysis for propeller turbine simulation was carried out by *Adanta et al*., [13] and Monsalve *et al*., [14]. Wibowo *et al.,* [15] analyzed the optimal thrust value of the B4-70, Ka4-70, and Au4-59 propellers on tugboats with varying rake using CFD. The method used in this study could predict the thrust value accurately. The study on the effect of mesh type was performed by Abidin *et al.* [16] . This research was carried out to investigate the performance of B-series propellers due to differences in structured and unstructured mesh. The result showed that the use of unstructured mesh was more accurate than the structured mesh. Fan *et al.* [17] performed the unsteady flow simulation of open water propeller using sliding mesh approach. The result indicated that the time discretization format has a greater impact on thrust, but has almost no effect on torque. The approach used in the study was robust to predict the thrust. However, a small-time step should be considered in order to capture the vorticity accurately. A dynamic mesh approach on open water propeller with the multiphase solver were investigated by Masoomi and Mosavi [18]. The thrust coefficient, torque coefficient, and open water efficiency obtained from the approach were compared to the experiment data. The average error percentage was 7.5%. Similar to the method, a dynamic mesh was caried out in a single blade of the B-series propeller and other blades were performed by using a rotational periodicity (blade numbers) to save the computational time [19]. Another study regarding the CFD approach on propeller was performed by Bahatmaka and Kim [20] using arbitrary mesh interface (AMI) and multi reference frame (MRF) techniques. The numerical simulation results for both approaches were in good agreement with the experimental data according to the values of thrust and torque. Nevertheless, the MRF had a good result and could perform the best rotational velocity if compared to AMI in the same advance velocity. Next, Hang *et al*., [21] also used MRF to investigate the effect of propeller disc angle and advance ratio. The results show that the MRF used in the study could predict the aerodynamic characteristics of Low Reynolds Number propeller at different propeller disc angle.

In the present study, CFD simulation model for optimum design of B-series propeller is employed using Multiple Reference Frame (MRF). The MRF is proposed to predict the performance of the propeller. A preliminary optimization is applied to B-series propeller with the Non-dominated Sort Genetic Algorithm-II (NSGA-II) prior to the simulation. The optimization is addressed to find out the optimum design of B-series propeller for a given initial condition. The thrust coefficient and open water efficiency are maximized in the optimization process which are then subjected to constraint function imposed by required thrust. The optimization is carried out to blade number Z=3 and Z=5 in order to provide various optimum solutions for each blade number. The population of design space is obtained after running the optimization program. The final optimum design parameter is considered using crowding distance value in the population. The thrust values generated by optimum design will be predicted using MRF and be compared to those obtained from optimization program.

2. Methodology
2.1 Non-dominated Sort Genetic Algorithm-II (NSGA-II) for B-series Optimization

The multi objective problem on propeller design optimization can be solved by formulating the objective functions and subjecting to constraint function. The performance characteristics of the B-series were reported by Oosterveld *et al.,* [22]. The open water characteristics in the form of thrust coefficient (K_T) and torque coefficient (K_Q) under the Reynolds number 2×10^6 condition which was then written into the following equation.

$$K_T = \sum_{n=1}^{39} C_{s,t,u,v} \, (J)^s \left(\frac{P}{D}\right)^t \left(\frac{A_E}{A_O}\right)^u (Z)^v \qquad (1)$$

$$K_Q = \sum_{n=1}^{47} C_{s,t,u,v} \, (J)^s \left(\frac{P}{D}\right)^t \left(\frac{A_E}{A_O}\right)^u (Z)^v \qquad (2)$$

$$\eta_O = \frac{J}{2\pi} \frac{K_T}{K_Q} \qquad (3)$$

where J, P/D, A_E/A_O, η_O are the advance coefficient, pitch ratio, expanded area ratio, blade number, and open water efficiency respectively. *C, s, t, u, v* are the polynomial coefficients given in tabular form [22] . Mathematically, the problem in B-series propeller optimization can be written as follows.

Maximize:

$$f_1(x) = f(K_T)$$

$$f_1(x_i, \ldots, x_n) = f\left(\sum_{n=1}^{39} C_{s,t,u,v} \, (J)^s \left(\frac{P}{D}\right)^t \left(\frac{A_E}{A_O}\right)^u (Z)^v\right) \qquad (4)$$

$$f_2(x) = f(\eta_O)$$

$$f_2(x_i, \ldots, x_n) = f\left(\frac{J}{2\pi} \frac{K_T}{K_Q}\right) \qquad (5)$$

Subjected to thrust constraint:

$$f_1 = \left(\frac{R_T}{\rho \, D^2 (1-t) \, (1-w)^2 V_S{}^2} J^2\right)$$

$$f_1 - \left(\frac{R_T}{\rho \, D^2 (1-t) \, (1-w)^2 V_S{}^2} J^2\right) = 0 \qquad (6)$$

The f_1 and f_2 are the objective functions which have x_n solutions. The values of J, P/D, A_E/A_O are the desired solutions. Those variables can be represented as x_1, x_2, and x_3. Each solution has the lower and upper bound regarding to the B-series design range. The range of those variables is written as follows.

$$0 \leq x_1 \leq 1.8 \qquad , x_1 = J \qquad (7)$$
$$0.5 \leq x_2 \leq 1.4 \qquad , x_2 = \frac{P}{D} \qquad (8)$$
$$0.3 \leq x_3 \leq 1.05 \qquad , x_3 = \frac{A_E}{A_O} \qquad (9)$$

The number of blades (Z) is set to be discrete variable with values 3 and 5. The optimization process is carried out for each number of propeller blades within the B-series design range. Some of the procedures which distinguish NSGA-II from conventional genetic algorithms are the presence of fast-non-dominated sort, crowding distance, and crowded comparison operators. The purpose of the NSGA-II algorithm is to improve the adaptive fit of the population of candidate solutions for a Pareto frontier bounded by the constraint of the objective functions. The population will be sorted into a sub-population hierarchy based on the order of Pareto dominance. In contrast to genetic algorithms

in general, multi-objective optimization with NSGA-II tries to find as many elements of the Pareto set as possible. Therefore, the NSGA-II is equipped with an operator that can find out the level of a solution which is not dominated by other solutions so that it is able to explore the feasible region widely. The detail algorithm of NSGA-II was discussed by Deb *et al.,* [23]. Briefly, the general schematic of the NSGA-II is represented in the Figure 1.
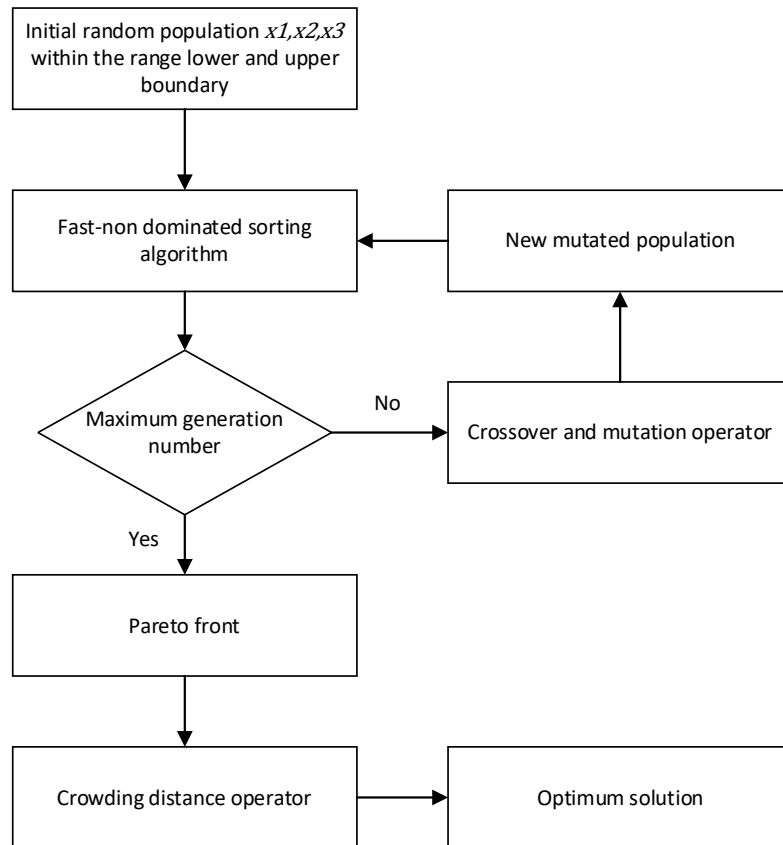
Fig. 1. General Schematic of the NSGA-II

Figure 1 depicts how the NSGA-II process run. First, the initial population is generated randomly within the range of lower and upper limit of variables x_1, x_2, and x_3 in one set of arrays. The fast-non-dominated sorting approach is employed to obtained the Pareto front which consists of non-dominated individuals. The main loop will be stop after reaching the maximum number of generations. The crowding distance of the Pareto front is then calculated to observe the density of one individual between another. The higher the crowding distance, the better fitness value of the individual. While the maximum generation is not reached the program will execute the crossover and mutation operator with the certain probability value to generate the new population. Some set up values for NSGA-II in this study is summarized in the Table 1. The maximum generations are set to be 1000 with the total population of 500. The crossover probability is set to be 0.8 for each blade number.

Table 1
Set up values for NSGA-II

Parameters	Values
Maximum generations	1000
Populations	500
Crossover probability	0.8

The optimization was performed with some initial condition regarding to the ship's requirements. The ship main characteristic of the ship and the initial propeller characteristics are presented in Table 2. The diameter of the propeller that will be optimized was fixed as the initial diameter. The required thrust was used as constraint function which must be satisfied by the optimum propeller generated using NSGA-II program.

Table 2
Ship's main characteristics and the initial propeller

Parameters	Values
Length of Overall (LOA)	60.00 m
Length of Waterline (LWL)	56.50 m
Breadth (B)	8.10 m
Depth (D)	4.95 m
Draught (T)	2.60m
Vessel Speed (Vs)	27.00 knots
Propeller Type	Twin Screw
Propeller Diameter (Dp)	1.90 m
Blade Number (Z)	5
Required Thrust (T req.)	170.01 kN

2.2 Multi Reference Frame (MRF) Approach

The Multi Reference Frame (MRF) is one of CFD approaches for rotating body case. The MRF has capability to solve the rotating body flow in steady state. Hence, this method is feasible to predict the total thrust value generating by propeller in steady state. In this study, the robustness of this method in solving the flow of optimum propeller is investigated. The simple model, 3-blades propeller, and the complex one, 5-blades propeller, obtained from optimization process are used. The thrust value generating by those propellers will be compared with the optimization results. In this technique, the entire region of computational domain is sub-divided into one or more rotating region and one stationary region. This method allows the rotation of wall (impeller/propeller blade) without moving the mesh by introducing some changes in momentum equation. The governing equation of the flow over a propeller is expressed using the incompressible Navier-Stokes equation.

$$\nabla.(\rho u) = 0 \tag{10}$$

$$\nabla.(\bar{u}.\bar{u}) - \nabla.(\nu \nabla \bar{u}) = -\nabla \bar{p} + \nabla.(\overline{u'u'}) \tag{11}$$

Where $\bar{u}$ is the component of Reynolds-averaged velocity, p is value of pressure, and $\overline{u'u'}$ is the Reynold stress tensor. In MRF approach some source terms are introduced in the rotating regions of computational domain in order to solve one set of the equation for the entire domain. The Eq. (11) with the additional source terms is written as follow.

$$\nabla.(\bar{u}.\overline{u_r}) - \nabla.(\nu\nabla\bar{u}) = -\nabla\bar{p} + (\Omega \times \bar{u})$$ (12)

The convective term contains the relative velocity and the absolute velocity. The absolute velocity is the velocity field with respect to inertial frame (stationary region) $\bar{u}$ while the relative velocity in the rotating regions is $\overline{u_r}$. The Ω in Eq. (11) is the rotation speed. The momentum equation is solved for absolute velocity with convective fluxes which accounts for the rotation and rotating regions by making fluxed relative to the stationary frame in all regions.

2.3 CFD Setup

The optimum design parameters are used to design the 3D model of propeller which will be analyzed using CFD simulation. It is carried out to determine the thrust value of each optimum propeller numerically. In this study, the simulation is performed in open water condition. The steady MRF approach is applied to solve the governing equation. The unstructured mesh is generated within computational domain. The computational domain and the generated mesh are shown in Figure 2 and Figure 3 respectively.
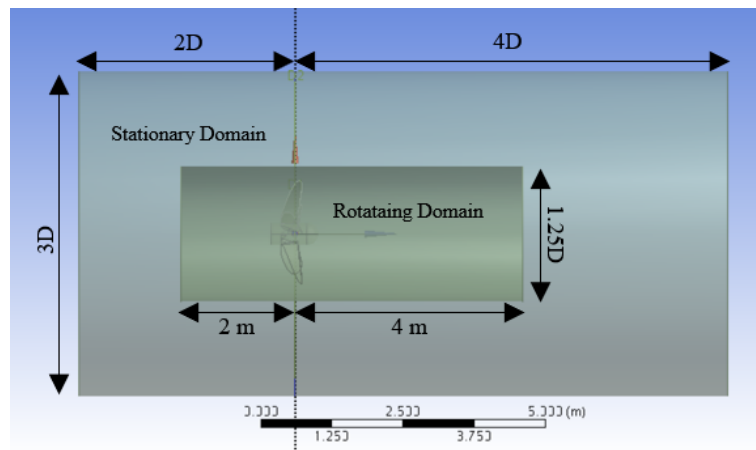
Fig. 2. Computational domain for open water simulation

In the MRF approach the domain was divided into two regions which are stationary region and the rotating region representing the flow due to rotating propeller at certain speed. The second order scheme was used to discretize the convective terms. The inlet boundary with an input value of incoming flow (Va) is imposed, a static pressure was applied as outlet boundary, and no slip wall was imposed to the wall. In addition, the $k - \varepsilon$ turbulence model is used with scalable wall function. Besides, the rotating domain velocity is set using the propeller speed obtained from optimization which is contributed by advance coefficient (J). In addition, wall boundary in the form of no slip wall was imposed. The two fluid domains were then connected by fluid interface with the frame change of frozen rotor. The simulation reached the convergence after all of residuals dropped to the power of 10^{-5}.
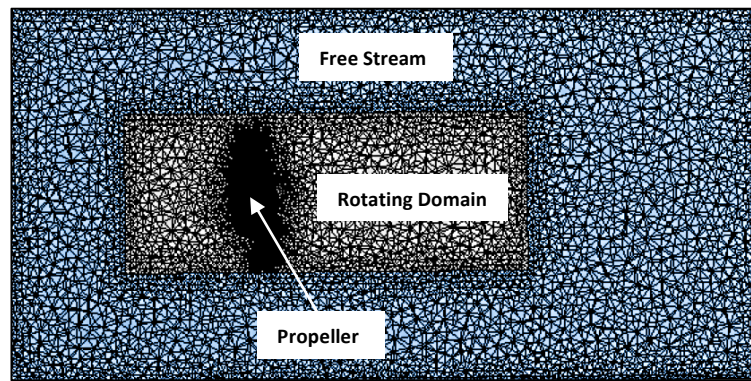
Fig. 3. Unstructured Mesh

3. Results
3.1 Optimum Solutions

This section discusses the results obtained from the optimization process by NSGA-II. The specified objective functions are f_1 and f_2 according to Eq. (4) and (5). The constraint function is written in accordance with equation (6) and the solutions are bounded according to Eq. (7), (8), and (9). The optimization program was executed three times for each blade numbers to investigate the variations of the result obtained by the algorithm. The thrust values generated by each individual in the population were compared with the required thrust. The difference of those values was then used to calculate the mean square error (MSE) of each result from executing the program. Therefore, there are three populations result with each MSE values for blade number Z=3 and Z=5. The population with the smallest MSE value was selected to be compromise solution. The population result for blade number Z=3 and Z=5 are shown in Figure 4(a), (b), (c), and Figure 5(a), (b), (c) respectively.

From Figure 4 and Figure 5 it can be seen that after executing the NSGA-II for three times the generated population for each blades number are dissimilar. In order to analyze the data distribution of the populations, the error between thrust values generated by each individual in the population were compared with the required thrust. The error value was then identified its distribution. The distribution identification of the error was performed using statistics tool. The population with the smallest MSE is selected prior to the identification because the small MSE indicates that the population has preferable fitness value. The overall MSE values of each population are summarized in Table 3.

Table 3
MSE values of each population

N-Execution	MSE of Z=3	MSE of Z=5
Run 1	4.45×10^{-7}	4.01×10^{-7}
Run 2	4.27×10^{-7}	4.42×10^{-7}
Run 3	4.86×10^{-7}	3.82×10^{-7}

From the result, the population of Z=3 with the smallest MSE was obtained from Run 2 while the smallest MSE of Z=5 is achieved from Run 3. As a result, the population is selected to be identified its error distribution. The individual distribution of the population is shown in Table 4.

Table 4
Individual distribution of the population

Population	Distribution	p-value
Z=3 (Run 2)	Johnson Transformation	0.895
Z=5 (Run 3)	Johnson Transformation	0.883

(a)

(b)

(c)
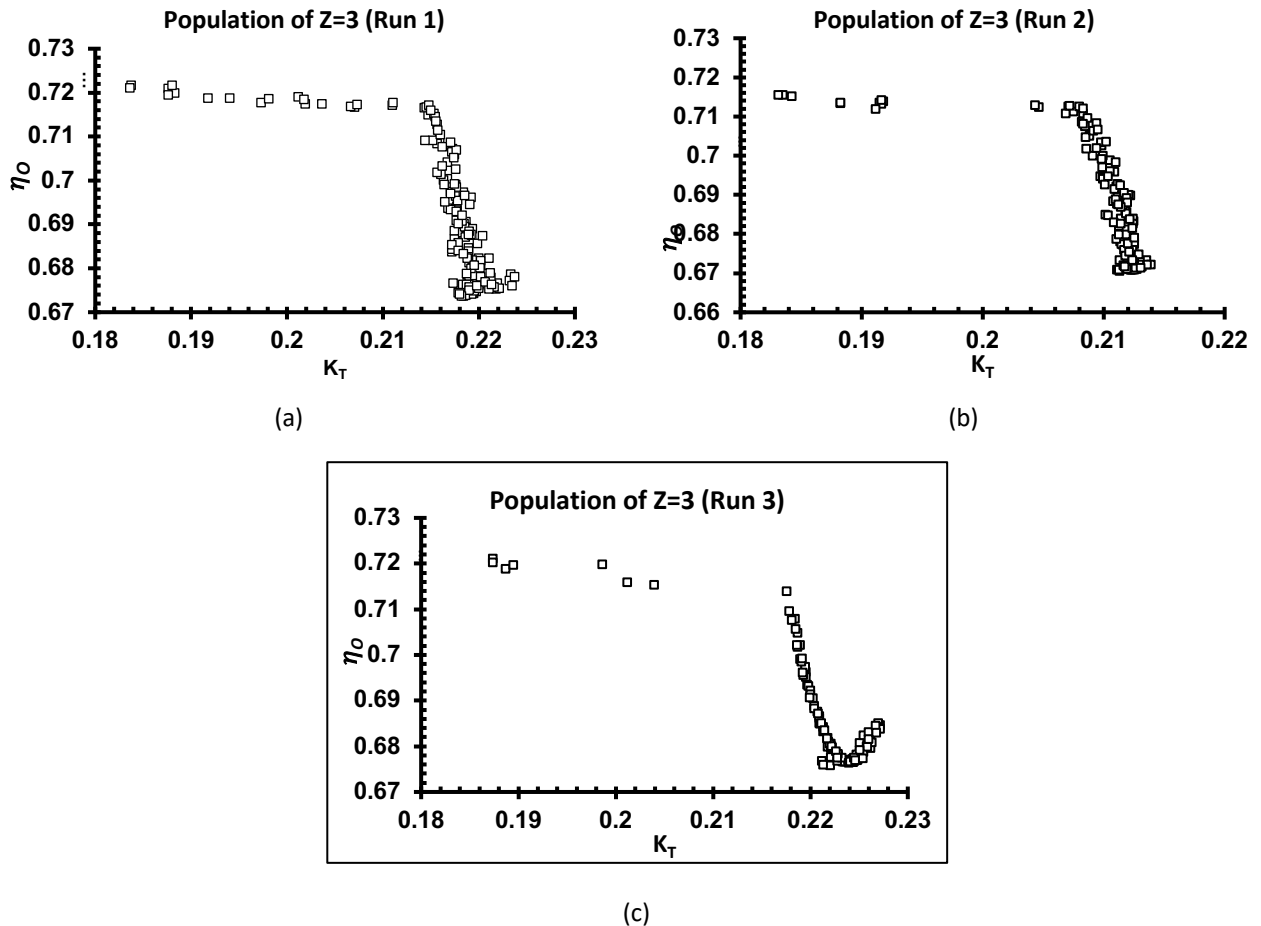
Fig. 4. Population of Z=3 (a) Run 1 (b) Run 2 (c) Run 3

Table 4 shows that the population of Z=3 and Z=5 have the same distribution error, namely, Johnson Transformation. Hence, the selected population are consistent and feasible to be used as optimum propeller design. The feasible individual within the population was selected more strictly afterwards using crowding distance. The crowding distance represents the density value between one individual and another in the same Pareto front. This value is used to determine the optimum individual on each Pareto front. As shown in the design space for each blade number, there are several individuals which are stated as feasible solution for optimum design. However, it is not obvious enough to decide which one to be selected as feasible solution. Therefore, the individuals existing in the design space need to be sorted according to their rank in the same Pareto front and the order of the rank is based on their crowding distance value. The results of the crowding distance value and the ranking value for each individual within the population are presented in Table 5.

(a)

(b)

(c)
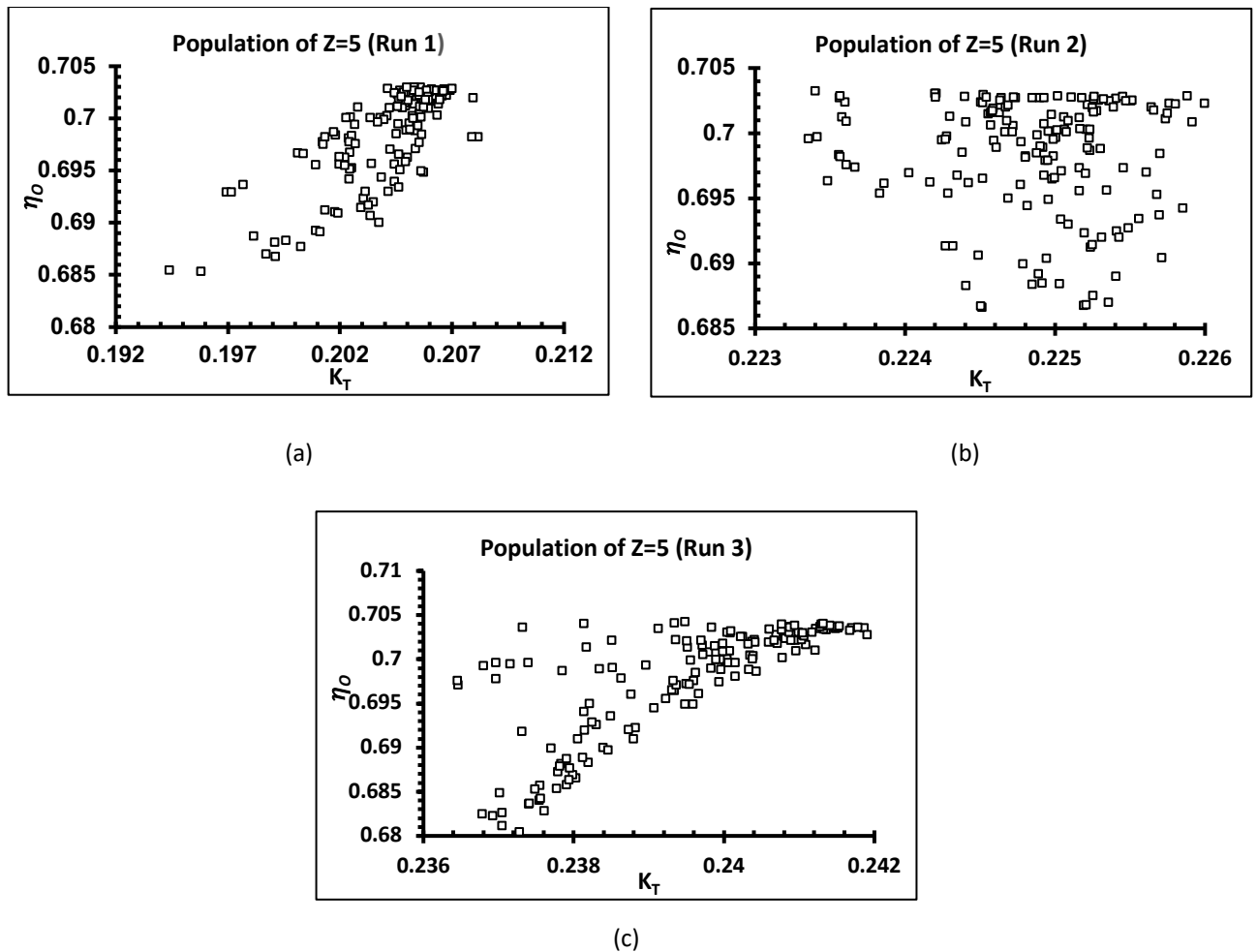
Fig. 5. Population of Z=5 (a) Run 1 (b) Run 2 (c) Run 3

Table 5
Crowding distance values

Z	Solution	x_1(J)	x_2(P/D)	x_3(A$_E$/A$_O$)	f_1(K$_T$)	f_2(η_O)	Crowding Distance
3	K$_T$ maximum	0.9614	1.3578	0.787	0.2139	0.6832	-
	η_O maximum	0.8161	1.0778	0.314	0.1545	0.7235	-
	Simultaneous	0.9583	1.3615	0.560	0.2125	0.6832	0.3937
5	K$_T$ maximum	1.0223	1.3998	0.416	0.2419	0.7028	-
	η_O maximum	1.0222	1.3991	0.501	0.2413	0.7040	-
	Simultaneous	1.0225	1.3994	0.476	0.2418	0.7036	0.7028

   Table 5 shows that the solution with the maximum K_T and the maximum η_O are the global maxima which have only a maximum value on one of the objective functions. Hence, the crowding distance of these individuals are infinity. The simultaneous solutions are those which have the optimum value on the overall objective functions simultaneously. The crowding distance values of these individuals are relatively high compared to the surrounding individuals. As a result, three propeller design parameters are obtained for each blades number. The 3D models were designed based on those parameters. For instance, the B3-787 represents the propeller design with blades number Z=3 and blade area ratio A$_E$/A$_O$=0.787. The optimum design of Z=3 and Z=5 are shown in Figure 6(a), (b), (c), and Figure 7(a), (b), (c) respectively.
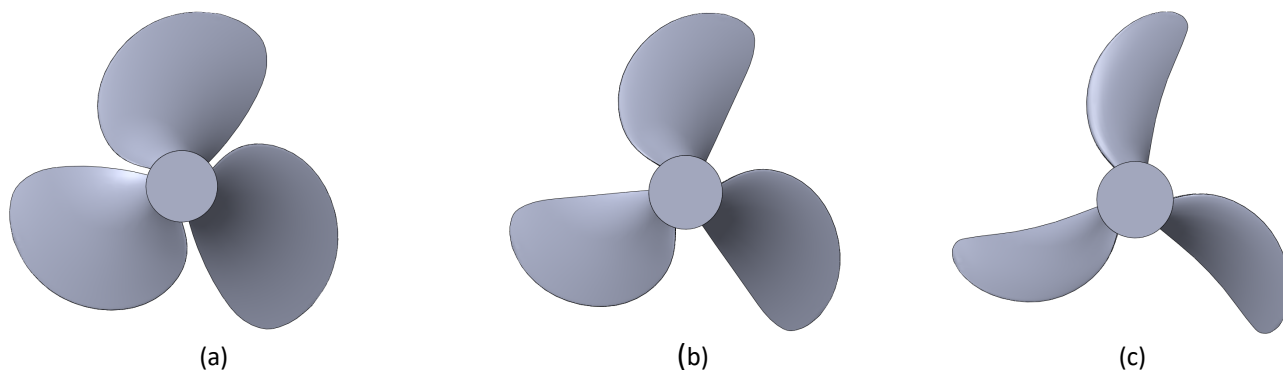
Fig. 6. Optimum Design of Z=3 (a) B3-787 (b) B3-560 (c) B3-314
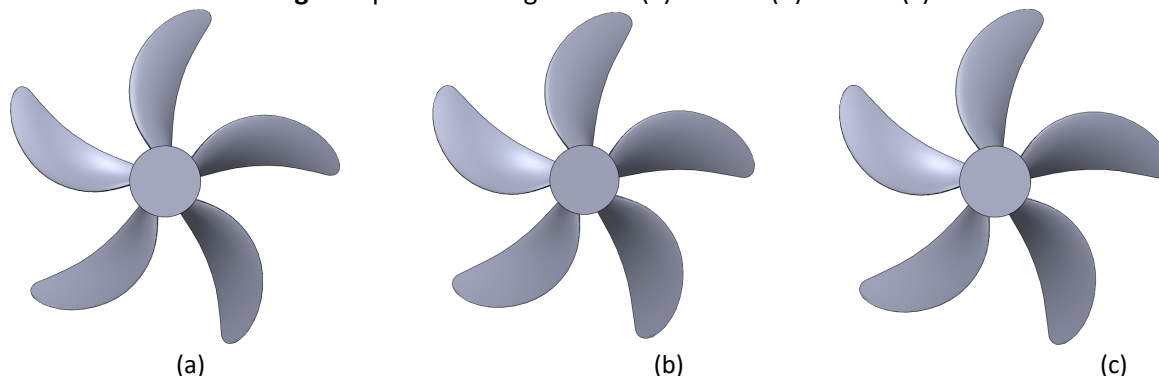
Fig. 7. Optimum Design of Z=5 (a) B5-416 (b) B5-501 (c) B5-476

3.2 CFD Results

The characteristic of each optimum propellers was investigated using MRF approach. The thrust value generated by the propeller was monitored in order to observe the convergence during the computation. The evolution of the thrust during the iteration is shown in Figure 8. The figure indicates that the computation was converged which was denoted by the constant thrust throughout the iterations. The results showed that six propeller models simulated using MRF could converge in short time.
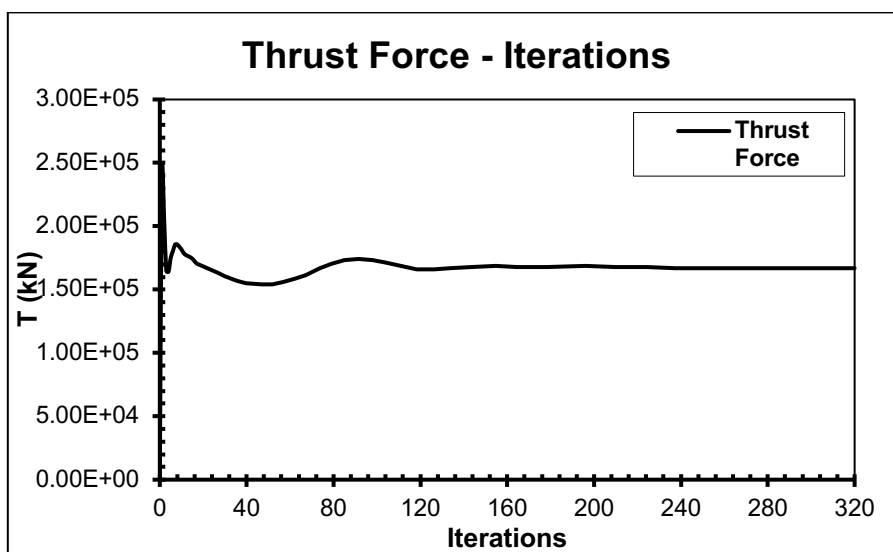
Fig. 8. Thrust Force Convergence

The flow passing through the propeller can be visualized using post processor. The velocity streamline generated by model Z=3 and Z=5 are presented in Figure 9(a), (b), (c), and Figure 10(a), (b), (c) respectively. The streamline depicts the flow due to the rotating propeller. It can be seen that the streamline followed the pitch distribution of the propeller blade. The model B3-787 and B3-314 generates more hub vorticity while the model B3-560 seemed to generate less hub vorticity. The wake of all B3 models showed that the flow behind the propellers is not uniform. Theoretically, the propeller wake of the model is not uniform due to the sectional profiles of the blade which vary along the propeller radius (r/R) as well as the pitch angles along the propeller blade induced different attack angle of the incoming flow. As a result, the wake behind the propeller is not uniform particularly at every propeller radius (r/R). This phenomenon is well-represented by the MRF method applied in this study.

The flow over the B5 models looked similar because the design characteristic of those models is identical. However, the model B5-416 generated less hub vorticity and its wake is relatively more uniform. From the result, the MRF approach is able to solve the flow passing through the propeller accurately.

(a)

(a)

(b)

(b)

(c)
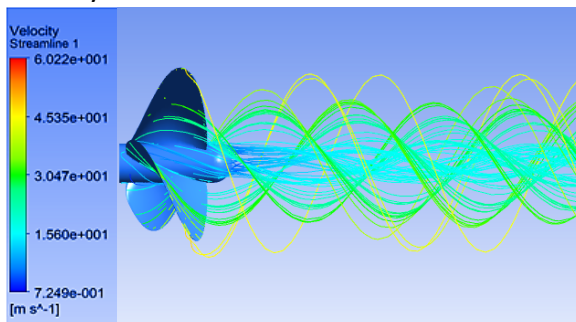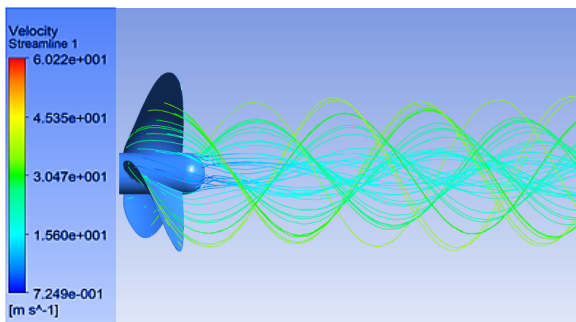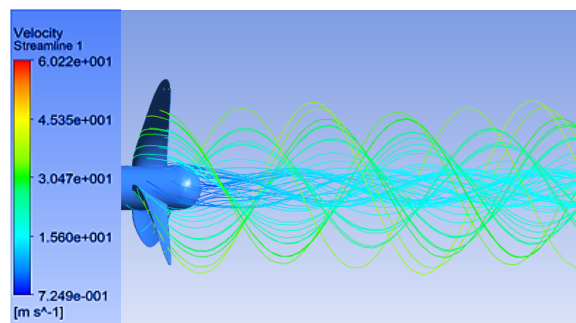
(c)

Fig. 9. Velocity Streamline of Z=3
(a) B3-787 (b) B3-560 (c) B3-314
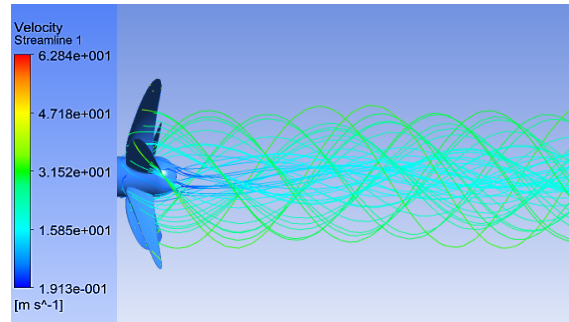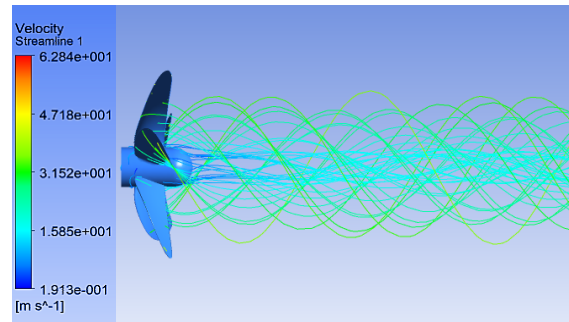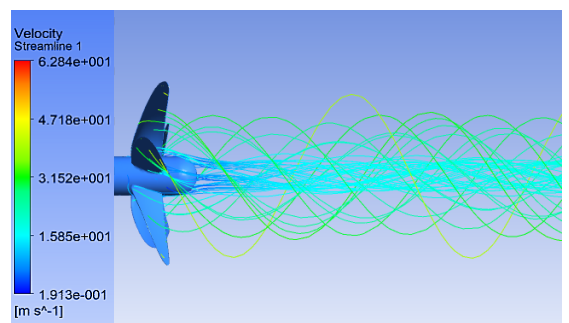
Fig. 10. Velocity Streamline of Z=3
(a) B5-416 (b) B5-501 (c) B5-476

The pressure distributions on the B3 and B5 models are presented in Figure 11(a), (b), (c), Figure 12(a), (b), (c), Figure 13(a), (b), (c), and Figure 14(a), (b), (c), respectively. The results indicated that the low pressure distributions are located on the face side of the propeller blades. On the other hand, the high pressure distributions are located on the back side of the propeller blades. As a result, there is pressure jump between those two sides. The difference of the pressure will magnify the total thrust force. For instance, the high pressure is distributed more on the back side of model B3-787 compared to the other two models. Hence, the pressure jump on this model is higher. The total thrust force is the difference of the pressure multiplied by the blade area. Therefore, the total thrust force of this model is relatively high since this model has wide blade area.

(a)

(a)

(b)

(b)

(c)

(c)
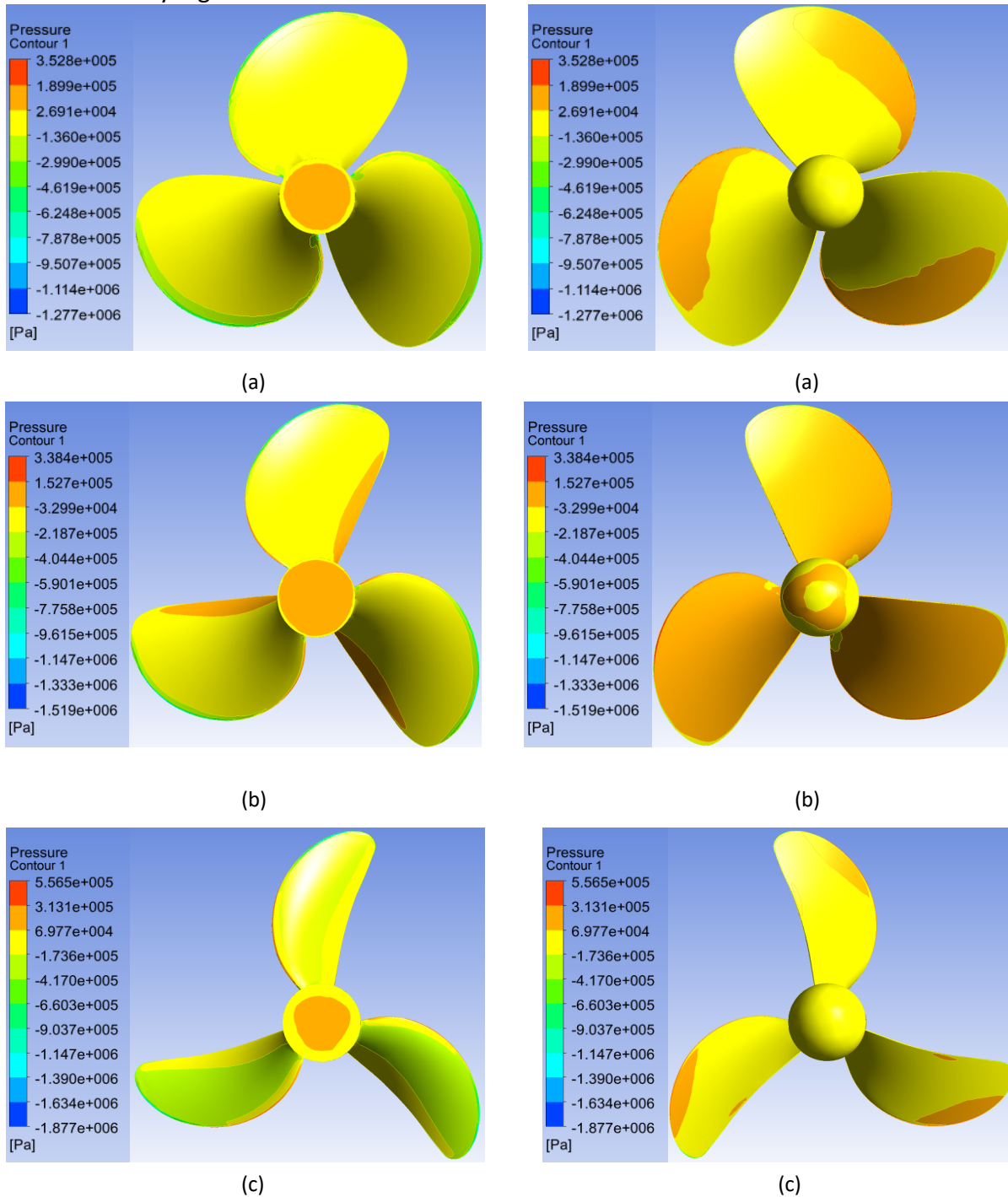
Fig. 11. Pressure Distribution on Face Side of Z=3 (a) B3-787 (b) B3-560 (c) B3-314

Fig. 12. Pressure Distribution on Back Side of Z=3 (a) B3-787 (b) B3-560 (c) B3-31
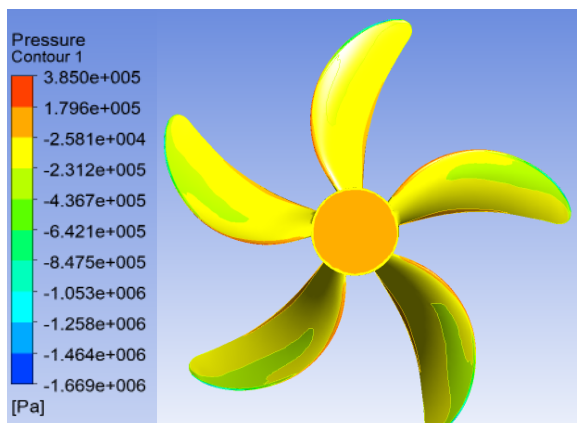
(a)
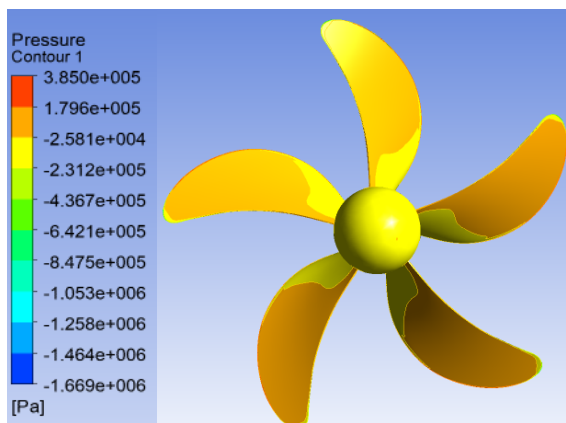
(a)
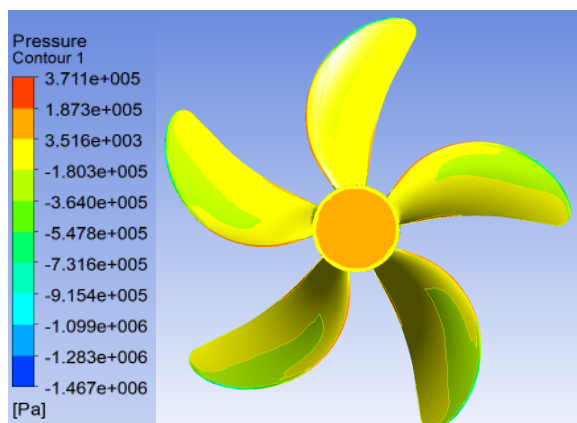
(b)
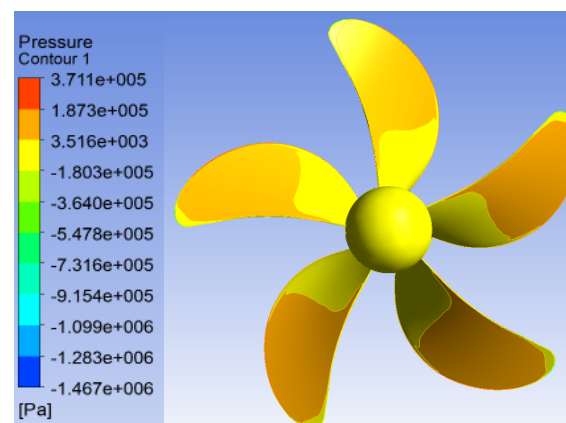
(b)
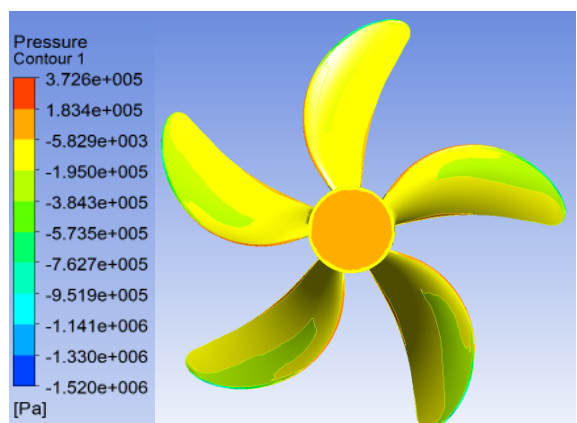
(c)
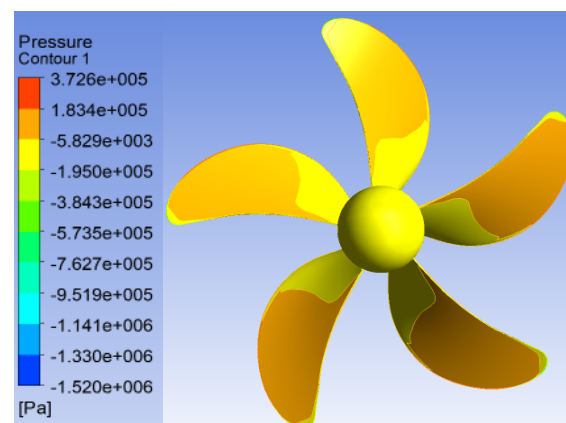
(c)

Fig. 13. Pressure Distribution on Face Side of Z=5 (a) B5-416 (b) B5-501 (c) B5-476

Fig. 14. Pressure Distribution on Back Side of Z=5 (a) B5-416 (b) B5-501 (c) B5-476

The results of B5 model showed the identical pressure distribution on the face and back side since the three models are not significantly different. Hence, the total thrust forces of those three models are quite similar. The overall results obtained from CFD simulation are summarized in Table

6 as well as the error value compared to the optimization results. The cell numbers generated for each model are also presented in the table. It showed that the total iteration for one simulation is about 300 up to 450 iterations. It indicates that the MRF approach can reach the convergence faster. In addition, the MRF indeed could solve the flow over the complex rotating body such as in model B5. The models consist of five blades which the geometry more complex than B3 model. However, the MRF is able to deal with that complexity of rotating flow over B5 model in fast convergence rate. Hence, this approach is adequate to reduce the computation time even for complex rotating body. In addition, the results obtained by this approach are consistent and accurate denoted by the difference thrust values between optimization results and CFD results which are under 6%. The comparison of thrust value obtained by MRF approach and optimization process are also presented in bar chart as shown in Figure 15 and Figure 16.

From the results, the MRF applied on both models, B3 and B5, can obtain the accurate solution in terms of thrust value. All results are very similar and consistent with those obtained from the optimization process. Furthermore, the pressure jump phenomenon are also well-represented by this method. After using the MRF, the results showed that the MRF not only robust in predicting the thrust value but also in representing the flow behind the propeller, both in simple model, 3-blades propeller, and the complex model, 5-blades propeller.

Table 6
Simulation results

Z	Model	Cell Numbers	Stop I = n	Thrust CFD (kN)	Thrust Opt. (kN)	Error (%)
3	B3-787	3,695,787	413	172.38	171.10	0.74
	B3-560	4,312,935	336	160.87	170.64	4.71
	B3-314	4,342,069	314	162.57	170.61	5.73
5	B5-416	5,314,284	321	167.11	170.47	1.97
	B5-501	5,554,575	319	168.80	170.53	1.02
	B5-476	5,626,895	319	168.34	170.03	0.99
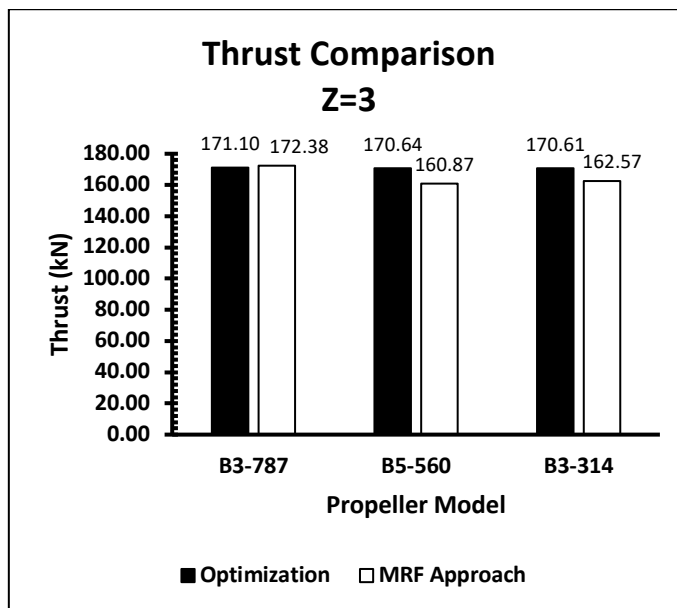
Fig. 15. Thrust Comparison of B3 Models
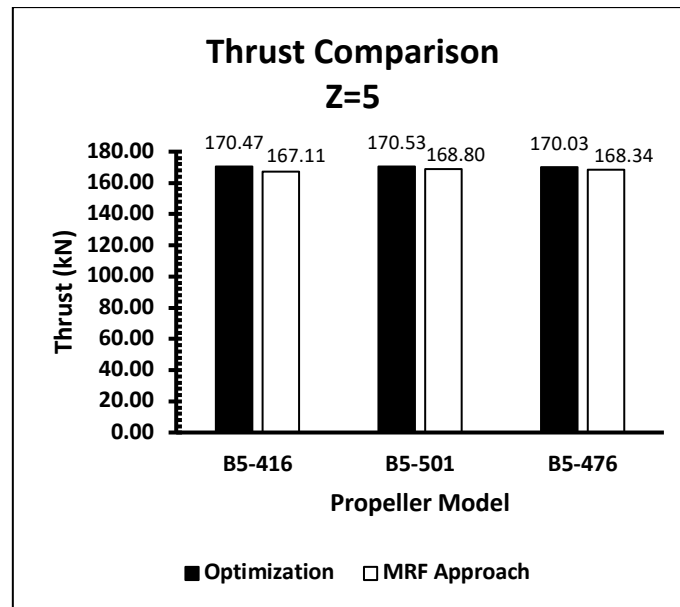
Fig. 16. Thrust Comparison of B5 Models

4. Conclusions

The multi objective optimization performed by NSGA-II is able to generate population consisting the feasible solutions. Hence, the optimum design of propeller can be obtained by multi objective optimization process. In this study, a preliminary optimization is applied to B-series propeller with the Non-dominated Sort Genetic Algorithm-II (NSGA-II). The purpose of this study is to find out the optimum performance of B-series propeller. The thrust coefficient and open water efficiency are maximized in the optimization process which are subjected to constraint function imposed by required thrust. The optimization is carried out to blade number Z=3 and Z=5. The population of design space is obtained after running the optimization program. The final optimum design parameter is considered using crowding distance value in the population. The result obtained by NSGA-II showed that the optimum design for Z=3 are B3-787, B3-314, B3-560, and Z=5 are B5-416, B5-501, B5-476 respectively. In addition, the Computational Fluid Dynamics analysis (CFD) is employed to investigate the characteristic of each propeller model by using Multi Reference Frame (MRF) approach. From the results, the MRF approach was able to solve the flow over rotating propeller consistently and accurately in fast convergence rate. The CFD results showed that the highest thrust value of the Z=3 is 172.38 kN generated by the B3-787 whereas the highest thrust value of Z=5 is 168.80 kN generated by the B5-501 model.

References
[1]   Esmailian, Ehsan, Hassan Ghassemi, and Hassan Zakerdoost. "Systematic probabilistic design methodology for simultaneously optimizing the ship hull–propeller system." *International Journal of Naval Architecture and Ocean Engineering* 9, no. 3 (2017): 246-255. https://doi.org/10.1016/j.ijnaoe.2016.06.007
[2]   Ghassemi, Hassan, and Hassan Zakerdoost. "Ship hull–propeller system optimization based on the multi-objective evolutionary algorithm." *Proceedings of the Institution of Mechanical Engineers, Part C: Journal of Mechanical Engineering Science* 231, no. 1 (2017): 175-192. https://doi.org/10.1177/0954406215616655
[3]   Jiang, Jingwei, Haopeng Cai, Cheng Ma, Zhengfang Qian, Ke Chen, and Peng Wu. "A ship propeller design methodology of multi-objective optimization considering fluid–structure interaction." *Engineering Applications of Computational Fluid Mechanics* 12, no. 1 (2018): 28-40. https://doi.org/10.1080/19942060.2017.1335653

[4]   Benini, Ernesto. "Multiobjective design optimization of B-screw series propellers using evolutionary algorithms." *Marine technology and SNAME news* 40, no. 04 (2003): 229-238. https://doi.org/10.5957/mt1.2003.40.4.229

[5]   Xie, Guanmo. "Optimal preliminary propeller design based on multi-objective optimization approach." *Procedia Engineering* 16 (2011): 278-283. https://doi.org/10.1016/j.proeng.2011.08.1084

[6]   Gaafary, M. M., H. S. El-Kilani, and M. M. Moustafa. "Optimum design of B-series marine propellers." *Alexandria Engineering Journal* 50, no. 1 (2011): 13-18. https://doi.org/10.1016/j.aej.2011.01.001

[7]   Takekoshi, Yoshihisa, Takafumi Kawamura, Hajime Yamaguchi, Masatsugu Maeda, Norio Ishii, Koyu Kimura, Tadashi Taketani, and Akihiko Fujii. "Study on the design of propeller blade sections using the optimization algorithm." *Journal of marine science and technology* 10, no. 2 (2005): 70-81. https://doi.org/10.1007/s00773-005-0197-y

[8]   Ren, Li, and Wen Xiao Zhang. "Matching Optimization of Ship Engine and Propeller Based on PSO-GA Algorithm." In *Applied Mechanics and Materials*, vol. 121, pp. 4503-4507. Trans Tech Publications Ltd, 2012. https://doi.org/10.4028/www.scientific.net/AMM.121-126.4503

[9]   Darsono, Febri Budi, Rahmad Doni Widodo, and Akhmad Nurdin. "Analysis Of the Effect of Flow Rate and Speed on Four Blade Tubular Water Bulb-Turbine Efficiency Using Numerical Flow Simulation." *Journal of Advanced Research in Fluid Mechanics and Thermal Sciences* 90, no. 2 (2021): 1-8. https://doi.org/10.37934/arfmts.90.2.18

[10]   Arifin, Mohammad Danil, Frengki Mohamad Felayati, and Andi Haris Muhammad. "Flow Separation Evaluation on Tubercle Ship Propeller." *CFD Letters* 14, no. 4 (2022): 43-50. https://doi.org/10.37934/cfdl.14.4.4350

[11]   Prakoso, Aji Putro, Warjito Warjito, Ahmad Indra Siswantara, Budiarso Budiarso, and Dendy Adanta. "Comparison Between 6-DOF UDF and Moving Mesh Approaches in CFD Methods for Predicting Cross-Flow PicoHydro Turbine Performance." *CFD Letters* 11, no. 6 (2019): 86-96.

[12]   Adanta, Dendy, Budiarso Budiarso, and Ahmad Indra Siswantara. "Assessment of turbulence modelling for numerical simulations into pico hydro turbine." *Journal of Advanced Research in Fluid Mechanics and Thermal Sciences* 46, no. 1 (2018): 21-31.

[13]   Adanta, Dendy, Mochammad Malik Ibrahim, Dewi Puspita Sari, Imam Syofii, and Muhammad Amsal Ade Saputra. "Application of the Grid Convergence Index Method and Courant Number Analysis for Propeller Turbine Simulation." *Journal of Advanced Research in Fluid Mechanics and Thermal Sciences* 96, no. 2 (2022): 33-41. https://doi.org/10.37934/arfmts.96.2.3341

[14]   Cifuentes, Oscar Darío Monsalve, Jonathan Graciano Uribe, and Diego Andrés Hincapié Zuluaga. "Numerical Simulation of a Propeller-Type Turbine for In-Pipe Installation." *Journal of Advanced Research in Fluid Mechanics and Thermal Sciences* 83, no. 1 (2021): 1-16. https://doi.org/10.37934/arfmts.83.1.116

[15]   Wibowo, Gagah Prayogo, Deddy Chrismianto, and Berlian Arswendo Adietya. "Analisa Nilai Thrust Optimum Propeler B4-70, Ka4-70 Dan Au4-59 Pada Kapal Tugboat Pelabuhan Paket-Ii 2x1850hp Dengan Variasi Sudut Rake Menggunakan CFD." *Jurnal Teknik Perkapalan* 5, no. 1 (2017).

[16]   M. Z. A. Abidin, M. Z. A. Z. Abidin, and S. W. Adji, "Analisa performance ropeller B-series dengan pendekatan structure dan unstructure meshing," *Jurnal Teknik ITS* 1, no. 1 (2012): G241–G246.

[17]   Fan, Yang, Chen Kunpeng, Chen Weimin, and Dong Guoxiang. "The effect of time discretization on the propeller hydrodynamic performance simulation in self-propulsion and open water conditions." In *Journal of Physics: Conference Series*, vol. 1834, no. 1, p. 012008. IOP Publishing, 2021. https://doi.org/10.1088/1742-6596/1834/1/012008

[18]   Masoomi, Mobin, and Amir Mosavi. "The One-Way FSI Method Based on RANS-FEM for the Open Water Test of a Marine Propeller at the Different Loading Conditions." *Journal of Marine Science and Engineering* 9, no. 4 (2021): 351. https://doi.org/10.3390/jmse9040351

[19]   Fitriadhy, Ahmad, Nur Amira Adam, C. J. Quah, Jaswar Koto, and Faisal Mahmuddin. "CFD prediction of b-series propeller performance in open water." *CFD letters* 12, no. 2 (2020): 58-68.

[20]   Bahatmaka, Aldias, and Dong-Joon Kim. "The Influence of Meshing Strategies on the Propeller Simulation by CFD." *Journal of Advanced Research in Ocean Engineering* 4, no. 2 (2018): 78-85.

[21]   Hang, Leong Chee, Nur Athirah Nadwa Rosli, Mastura Ab Wahid, Norazila Othman, Shabudin Mat, and Mohd Zarhamdy Md Zain. "CFD Analysis on Propeller at Varying Propeller Disc Angle and Advance Ratio." *Journal of Advanced Research in Fluid Mechanics and Thermal Sciences* 96, no. 1 (2022): 82-95. https://doi.org/10.37934/arfmts.96.1.8295

[22]   Oosterveld, Marinus Willem Cornelis, and Peter van Oossanen. "Further computer-analyzed data of the Wageningen B-screw series." *International shipbuilding progress* 22, no. 251 (1975): 251-262. https://doi.org/10.3233/ISP-1975-2225102

[23]   Deb, Kalyanmoy, Amrit Pratap, Sameer Agarwal, and T. A. M. T. Meyarivan. "A fast and elitist multiobjective genetic algorithm: NSGA-II." *IEEE   transactions   on   evolutionary   computation* 6,   no.   2   (2002):   182-197. https://doi.org/10.1109/4235.996017